Vehicle System Dynamics
International Journal of Vehicle Mechanics and Mobility

ISSN: (Print) (Online) Journal homepage: https://www.tandfonline.com/loi/nvsd20

HIL simulation of high-speed train active stability employing active inertial actuators

Jun Cheng, Hongwei Yan, Xiangguang Zhang, Kang Chen & Yuan Yao

VEHICLE SYSTEM DYNAMICS
https://doi.org/10.1080/00423114.2022.2139727

Check for updates

HIL simulation of high-speed train active stability employing active inertial actuators

Jun Cheng[a], Hongwei Yan[a], Xiangguang Zhang[a], Kang Chen[a] and Yuan Yao [a,b]

[a]State Key Laboratory of Traction Power, Southwest JiaoTong University, Chengdu, People's Republic of China; [b]Yibin Research Institute, Southwest Jiaotong University, Yibin, People's Republic of China

ABSTRACT

To enhance the lateral stability of a certain type of high-speed train under bogie's active control, characteristics of inertial actuators that generate control force in the active control system are studied, the control delay of the whole Hardware-in-the-Loop (HIL) system is measured, and multi-objective optimisation for feedback parameters with or without the control delay is achieved in this study. A linear model of bogie lateral dynamics, with two inertial actuators, acting on the front and rear end beams, is established for the optimisation. Correspondingly, a nonlinear vehicle model is established in the Simpack platform for both mathematical simulation and HIL simulation to verify the control effects. As the force source of active control, dynamic characteristics of the inertial actuator with different control strategies are examined. Multi-objective optimal control is carried out on the linear active bogie models with and without the delay measured in the experiment to improve the bogie hunting stability. The control method is then evaluated in a nonlinear vehicle model and HIL simulation. Simulation results show that the lateral dynamic performance of the high-speed train can be effectively improved with the active stability system even with a large time delay.

ARTICLE HISTORY

Received 5 January 2022
Revised 6 October 2022
Accepted 19 October 2022

KEYWORDS

High-speed train; multi-objective optimisation; active control; time delay; HIL simulation

1. Introduction

With the continuous increase in the operating speed of a high-speed train, its vibration problem is intensified, which subsequently leads to the deterioration of the ride comfort and reduction of service life. Nowadays, the operating speed of high-speed trains has reached up to 350 km/h. The vehicle's dynamic performance under extreme wheel-rail contact conditions cannot be guaranteed with a traditional passive suspension system. In view of above situations, adopting active and semi-active control technology has become a potential research field for the new generation of high-speed train suspension. Numerous kinds of research have been implemented about the active and semi-active control in the suspension system of railway vehicles for a variety of purposes [1] such as minimising the flexibility effects that arise as a consequence of having lighter vehicles [2], adopting condition monitor for the monitoring of infrastructure and the rolling stock itself [3], improving

CONTACT Yuan Yao yyuan8848@163.com

the dynamic performance and riding quality of high-speed vehicles [4–10], improving the ride comfort and the safety [11] and using active wheelset method to improve both stability and performance in curve [12].

Apart from damping and stiffness, an inverter is found as a new component of suspension that can be properly applied to enhance the ride comfort of railway vehicles in the current research [13–15]. Inertial actuators developed based on active dynamic vibration absorbers are widely used in structural vibration engineering. It has the advantages of small external interference, a wide frequency band and high damping efficiency. Railway vehicle is able to take the advantage of the inertia of the laterally elastically suspended motor in a drive bogie. Braghin et al. designed a new type of low-frequency inertial actuator [16]. Compared with the traditional actuator, its telescopic rod is obviously longer and its working frequency is lower. Benassi and Elliott established the inertial actuator system model for active vibration isolation and studied the influence of inertial actuator displacement feedback and force feedback on control system performance [17,18]. Dal Borgo et al. conducted an experimental study on the nonlinear dynamics of the inertial actuator and found that the nonlinear dynamics of the actuator will affect the stability margin of the feedback loop when the velocity is fed back [19]. Basic linear model parameters of the actuator were determined by parameter identification methods in his research. Hou et al. put forward a method of installing inertial actuators on the front and rear end beams of the bogie frame and studied the active control strategies of bogie frame's lateral displacement and lateral velocity feedback [6]. Yao et al. studied the method of using an inertial actuator to mitigate the lateral vibration of the frame. Suspension parameters were optimised by a genetic algorithm [8]. The proposed method effectively improved the hunting stability of the bogie.

The research for the suspension system of railway vehicles usually needs to be validated by full-scale test rigs or on-track tests. However, full-scale test rigs and vehicle on-track tests are expensive and labour-consuming, especially for the design of the active suspension. As a relatively economical test method, the method of hardware-in-the-loop (HIL) simulation has been widely introduced in the design of railway vehicle parts [20–22]. In the process of railway vehicle HIL simulation, the studied physical hardware and a virtual model which can simulate the other parts of a vehicle are required. The simulation loop is run by the combination of the virtual part of the whole vehicle model and the real part of certain hardware under research [23]. Since some nonlinear components of suspension elements cannot be modelled and analysed by the statistic method, HIL simulation can be regarded as a relatively comprehensive method for its consideration of all characteristics of certain hardware.

Time delay is an inherent characteristic of an active control system. The delay leads to an undesired influence on the control effect most of the time and may even lead to the instability of the whole system. Yao et al. studied the robustness of optimised linear control under different time delays [8]. Although a stability margin will always be set, considering the characteristic of delay in the control system when designing the control strategy is a fundamental solution to eliminate the negative effect of time delay. Zhang et al. discussed the integral-inequality solution for the delay-dependent stabilisation and designed a kind of memoryless linear feedback controller [24]. Chen et al. established the statistic Takagi–Sugeno (T–S) fuzzy systems with input delay and discussed delay-dependent stabilisation conditions [25]. Shin et al. designed a controller for motorised vehicles considering dynamic friction and actuator delay and examined its performance in simulation

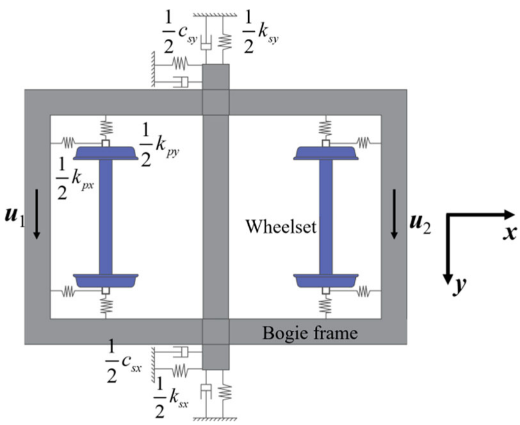

Figure 1. Theoretical bogie model.

[26]. Bideleh et al. studied H∞ control with a time delay compensator in an active steering bogie to improve stability and curving performance against track irregularity [27].

In this paper, the dynamic characteristics of a type of inertial actuator and its control strategy are studied. The optimisation for Proportional Integral Derivative (PID) control in a linear bogie model with delay is performed and then validated in the nonlinear vehicle model simulation and the inertial actuator in the HIL simulation. A linear single bogie model with the linear state feedback control considering the time delay is established for the control design. As a force element in active control, the dynamic characteristics and control strategies of the inertial actuator are studied by the experiment. To obtain the optimal parameters for PID control, a multi-objective optimisation problem with two objects of bogie lateral vibration is solved using the Non-dominated Sorting Genetic Algorithm-II (NSGA-II). The control effects and influence of delay are analysed. Finally, the optimised PID parameters are validated in co-simulation in the Simpack platform and HIL simulation.

2. Vehicle dynamics model

2.1. Bogie linear theoretical model

In this study, lateral stability is considered as optimisation objective. A 6-DOF bogie linear model, consisting of two wheelsets, one frame and two actuators, is established. Two inertial actuators are installed at the front and rear end beams of the bogie frame, which provide lateral control force on the bogie system. The feedback force generated by inertial actuators depends on the lateral vibration states of the bogie frame.

The bogie model is shown in Figure 1. Two wheelsets are coupled with the frame through primary longitudinal and lateral stiffness k_{px}, k_{py}. Since the mass of the car body is much larger than that of the bogie, it can be assumed that the lateral movement of the car body is always fixed. That is, in the proposed model, the bogie frame is directly connected with the ground through the secondary suspension k_{sx}, c_{sx}, k_{sy} and c_{sy}. States of the model include lateral displacement and yaw angle of the bogie frame, lateral displacement and yaw angle of the two wheelsets.

The bogie system can be defined as follows:

$$\mathbf{M}_\mathrm{b}\ddot{\mathbf{x}} + \mathbf{C}_\mathrm{b}\dot{\mathbf{x}} + \mathbf{K}_\mathrm{b}\mathbf{x} = \mathbf{we}(t)+\mathbf{Q} + \mathbf{Bu}(t) \tag{1}$$

where $\mathbf{x} = [y_{\mathrm{w1}},\varphi_{\mathrm{w1}},y_{\mathrm{w2}},\varphi_{\mathrm{w2}},y_\mathrm{f},\varphi_\mathrm{f}]^\mathrm{T}$, y_{w1}, φ_{w1}, y_{w2} and φ_{w2} are the lateral displacement and yaw angle of two wheelsets, y_f, φ_f are the lateral displacement and yaw angle of the bogie frame. $\mathbf{M}_\mathrm{b}$, $\mathbf{C}_\mathrm{b}$ and $\mathbf{K}_\mathrm{b}$ represent the mass, damping and stiffness matrix of the bogie, respectively. Matrix **w** is the stiffness vector of two wheelsets and **e**(t) represents wheel-rail disturbance caused by track irregularity, **we**(t) can be regarded as the input perturbation of the bogie system. **Q** is the creeping force under the assumption that the spin creep force of the wheelset is negligible. **Q** is regarded as a combination of a stiffness matrix $\mathbf{K}_\mathrm{r}$ and a damping matrix $\mathbf{C}_\mathrm{r}$. Which can be incorporated into the matrix **K** and **C** if the wheel-rail force is not studied. **B** represents the control influence matrix and **u**(t) is the control forces generated by two actuators. These matrices and vectors are listed in the Appendix. Values of parameters are determined regarding the model of a certain type of Electric Multiple Units (EMU).

The integrated system model can be expressed as follows:

$$\mathbf{M}_\mathrm{b}\ddot{\mathbf{x}} + \mathbf{C}_\mathrm{e}\dot{\mathbf{x}} + \mathbf{K}_\mathrm{e}\mathbf{x} = \mathbf{we}(t)+\mathbf{Bu}(t) \tag{2}$$

where $\mathbf{C}_\mathrm{e} = \mathbf{C}_\mathrm{b} + \mathbf{C}_\mathrm{r}$, $\mathbf{K}_\mathrm{e} = \mathbf{K}_\mathrm{b} + \mathbf{K}_\mathrm{r}$, $\mathbf{C}_\mathrm{r}$ and $\mathbf{K}_\mathrm{r}$ are equivalent stiffness and damping matrix derived from wheel-rail contact. $\mathbf{K}_\mathrm{r}$ represents the coefficient of displacement in the simplified expression of creep force, which is theoretically the cause of lateral displacement and yaw angle of wheelsets. $\mathbf{C}_\mathrm{r}$ varies with the operating speed v. As v increases, the damping coefficient decreases. When the energy consumption determined by $\mathbf{C}_\mathrm{e}$ is less than the input $\mathbf{K}_\mathrm{e}$, the system becomes unstable.

2.2. Multi-body system model

A nonlinear multi-body system dynamics model of a certain type of EMU is established in the Simpack code. Seven rigid bodies are contained in the model: four wheelsets, two bogies and one car body. Each wheelset is connected to the bogie by primary suspension including primary dampers and rotary joints. Bogies and car-body are coupled by secondary suspension including yaw dampers and air springs. The wheelset tread is S1002G, and the rail cant is 1:40. Compared with a common model, four more force elements are set on the end beams of two bogies. The force elements of actuators are set to be connected to Matlab/Simulink modules for statistic simulation and HIL simulation.

3. Dynamic characteristics and control strategies of an inertial actuator

3.1. Inertial actuator model

An inertial actuator is a type of active vibration absorber. Inertia is coupled with the controlled system by stiffness k_p, damping c_p and electromagnetic force F_a. Parameters k_p and c_p are inherent characteristics of the inertial actuator. The inertial actuator system can be defined as follows:

$$m_p\ddot{z} + c_p\dot{z} + k_p z = F_a \tag{3}$$

The transfer function between the displacement of inertial mass and the actuating force of actuators can be obtained by performing Laplace transform on both sides of the equation. The transfer function between z and F_a is as follows:

$$\frac{Z}{F_a} = \frac{1}{m_p s^2 + c_p s + k_p} = \frac{1}{m_p(s^2 + 2\xi_p\omega_p s + \omega_p{}^2)} \tag{4}$$

where ω_p is the natural frequency of the inertial actuator system and ξ_p is the damping ratio.

The value of F_a is calculated by the control algorithm according to the sensor data. The working principle of the inertial actuator is based on Maxwells basic electromagnetic theory, which is mainly composed of the Gaussian electric pass law, Faraday's electromagnetic induction law, Gaussian magnetic flux law and Ampere's loop law. The expression of F_a is as follows:

$$\begin{aligned} F_a &= \frac{\partial W}{\partial z}|_i = -\frac{2\pi\mu r N H_c h_m}{L} i = k_f i \\ k_f &= -\frac{2\pi\mu r N H_c h_m}{L} \end{aligned} \tag{5}$$

where W represents the magnetic work, z is the displacement of the inertia, μ is the magnetic permeability of air, r, L and h_m are parameters related to the structure of a permanent magnet, N is the number of coils, H_c is the coercivity of permanent magnet and i represents instantaneous current in the circuit. Since parameters μ, r, L, h_m, N and H_c are constant, it can be concluded that F_a is directly proportional to the value of instantaneous current, and the constant part can be integrated by a proportional coefficient k_f.

When the inertial actuator is oscillating, the inertial force will be generated by inertial mass and conducted to the base structure. The inertial force can be calculated as follows:

$$F_t = m_p\ddot{z} \tag{6}$$

And the transfer function can be defined as follows:

$$\frac{F_t}{F_a} = \frac{s^2}{s^2 + 2\xi_p\omega_p s + \omega_p{}^2} \tag{7}$$

According to a certain control method, the inertial mass is driven to oscillate and generate inertial force by changing the input current, the inertial force is applied to the controlled system as the active control force of the system (Figure 2).

3.2. Force-tracking control

As inertial actuators are used as force sources to provide active control force for the vehicle system, the force generated by the actuators must be as close as possible to the expected control force calculated by the controller. It is necessary to adopt the double-loop feedback

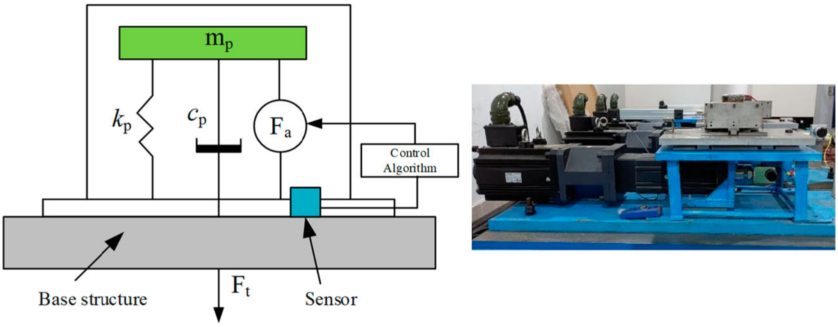

Figure 2. Inertial actuator and its test rig.

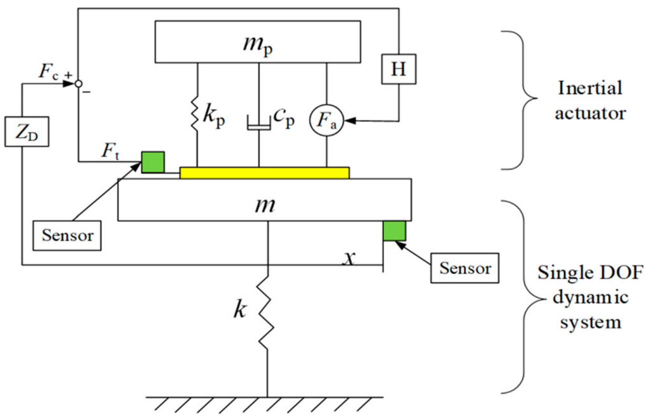

Figure 3. A dynamic model for force-tracking test.

control mode for the hardware-in-the-loop vehicle model, which contains the outer loop of the vehicle system combined with a controller and the inner loop of the actuator and its driver. The dynamic model used in the force-tracking test is shown in Figure 3.

In Figure 3, m_p is the mass of the inertial actuator, k_p and c_p are the stiffness and damping coefficient of the inertial actuator, respectively, the value of which is defined by the inherent characters of the actuator and acquired by parameter estimation. z_d indicates the transfer function from the displacement of the structure to the demanded control force F_c. F_c is then subtracted by the signal collected by the load cell between the inertial actuator and structure F_t, after which the signal passes through the transfer unit H and performs as the electromagnetic force F_a.

Three force-tracking strategies, including direct force feedback, integral force feedback and phase lag compensator, are tested on an inertial actuator by experiment. To prevent the actuator from hitting the stop end due to excessive driving force, the feedback force of the actuator is scaled.

3.2.1. Linear force feedback

When the direct force feedback strategy is adopted, the transfer function of the feedback loop can be expressed as follows:

$$H = h_f \tag{8}$$

where h_f represents the gain of the feedback system.

The larger h_f is set, the faster the force-tracking speed will be, but the larger h_f will also cause a larger overshoot and steady-state error of the active force.

3.2.2. Integral force feedback

The transfer function of integral force feedback can be defined as follows:

$$H = h_{if}/j\omega \tag{9}$$

where h_{if} is the feedback gain of integral force feedback.

Since integral feedback is only able to eliminate the drift after stabilisation, it has no good control effect on the decrease of rise time especially in the working condition of the high input frequency.

3.2.3. Phase lag compensator

To obtain a larger phase margin to enhance the static accuracy of the force-tracking loop, phase lag compensator feedback is taken into consideration. The transfer function of phase lag compensator feedback is as follows:

$$H = h_{pl}((j\omega + \omega_1)/j\omega) \tag{10}$$

where h_{pl} represents the control gain and ω_1 is the value of compensated phase shift.

The displacement curves of the mass in statistical simulation and experiment are shown in Figure 4(a), and the active control forces of which are shown in Figure 4(b).

It can be concluded that the control effect of linear force feedback is the best, while the force curves under the other two control methods deviate far from the required value according to Figure 4(b). The control force generated by the inertial actuator cannot track the given signal well under integral force feedback and phase lag compensator feedback. For the simple structure and small calculation amount of linear force feedback, it will be considered as the actuator inner loop strategy in HIL simulation in Section 6.

4. Time delay aimed optimisation

4.1. Time delay of an actuator

Time delay is an inevitable problem in the experimental study and practical application of active and semi-active control. The causes of a time delay could be the calculation time of the controller, conduction of the electric circuit, response time of motor drivers, dead zone of sensors, execution time of actuator force-tracking and other uncontrollable factors. The delay of the whole inertial actuator control system in this study can be measured by experiment as a total time delay in a black box. Since the current signal conducted to the driver of the inertial actuator is the output of the virtual part, and signals measured by

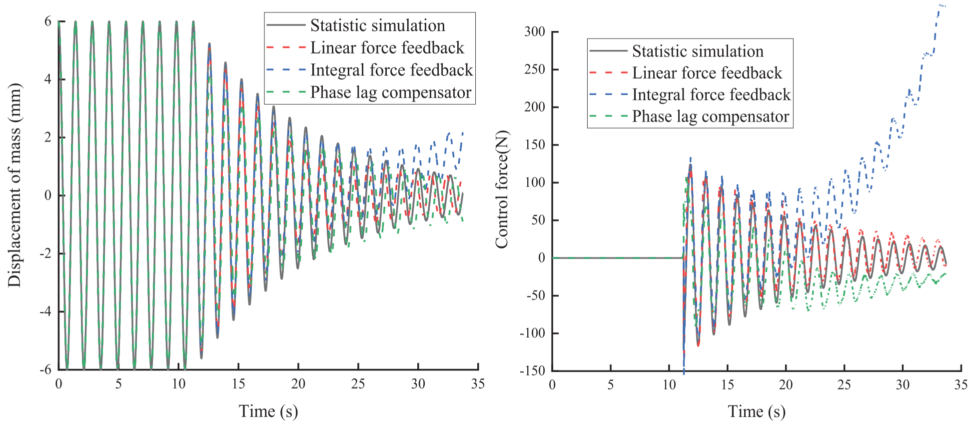

(a) Displacement of mass (b) Control force

Figure 4. Time-domain response of the inertial actuator with three different control strategies. (a) Displacement of mass; (b) Control force.

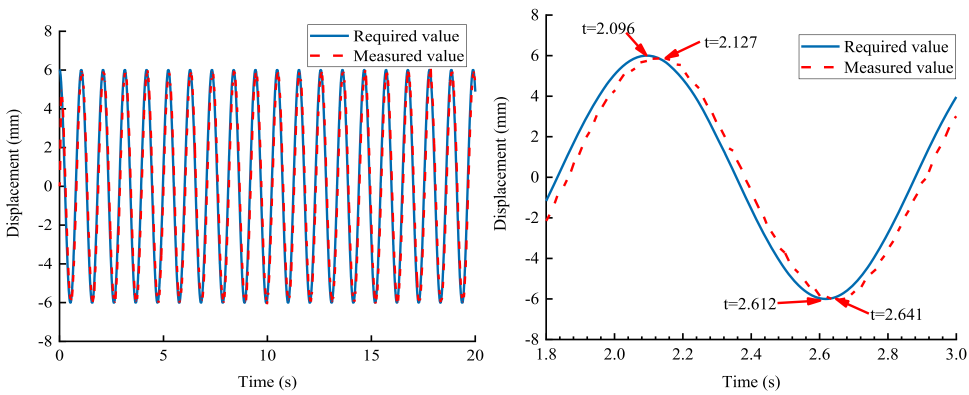

(a) Time-domain curves (b) Partial enlarged detail

Figure 5. The phenomenon of time delay in the experiment. (a) Time-domain curves; (b) Partial enlarged detail.

sensors are defined as the inputs, the delay in the whole hardware system can be regarded as the time difference between the outputs and inputs.

In an experiment, the input current signal of the inertial actuator is set as a series of the sinusoidal signal, and the measured signal is a sinusoidal signal lagging behind the input current. The time interval between two signal peaks is regarded as the time delay of the hardware system. The experiment results are shown in Figure 5.

Figure 5 shows the time-domain curves of the displacement signal calculated by the controller and measured by the sensor. Figure 5(b) shows the time delay in detail. According to the interval measured between peaks of two curves, the time delay of the whole control system in the following study can be 30 ms (Figure 6).

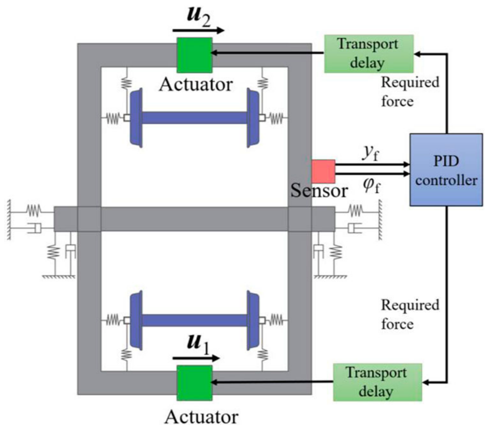

Figure 6. Sketch map of the bogie model combined with two PID modules.

4.2. Multi-objective optimal PID control design

A linear bogie theoretical model containing PID controller and control delay is established in Matlab/Simulink code. The German low interference spectrum is adopted for track irregularity, which is regarded as the outer excitation of the bogie system. The design purpose of the PID controller is to mitigate the lateral and yawing vibration of the bogie frame under excitation of track irregularity and the bogie hunting movement, such as to improve the hunting stability. Inputs of two PID controllers are set as the lateral displacement and yaw angle of the bogie frame, the outputs of which can be regarded as the required control force for the feedback loop. The force is subsequently generated by inertial actuators in the hardware part. A time delay block is set after the PID controller as the sum of delay in all components, which is measured as 30 ms. Considering the asymmetrical installation of two bogies in a vehicle model, the parameters k_p, k_i, k_d of both PID controllers are the same.

To obtain the minimum statistical values of lateral displacement and yaw angle of the frame, a multi-objective optimisation based on a genetic algorithm is adopted to optimise the control parameters k_p, k_i, k_d, which indicate the proportional gain, integral gain and derivative gain of PID control, respectively. The statistical values of lateral displacement y_s and yaw angle φ_s are defined as follows:

$$y_s = \bar{y} + 3 \times \sqrt{\frac{\sum_{i=1}^{n} (y_i - \bar{y})^2}{n}}$$

$$\varphi_s = \bar{\varphi} + 3 \times \sqrt{\frac{\sum_{i=1}^{n} (\varphi_i - \bar{\varphi})^2}{n}} \tag{11}$$

And the multi-objective optimisation problem can be stated as follows:

$$\min\{y_s, \varphi_s\} \tag{12}$$

According to the installation of two actuators, force in the same direction and torque in different directions will be generated at once when two actuators work at the same

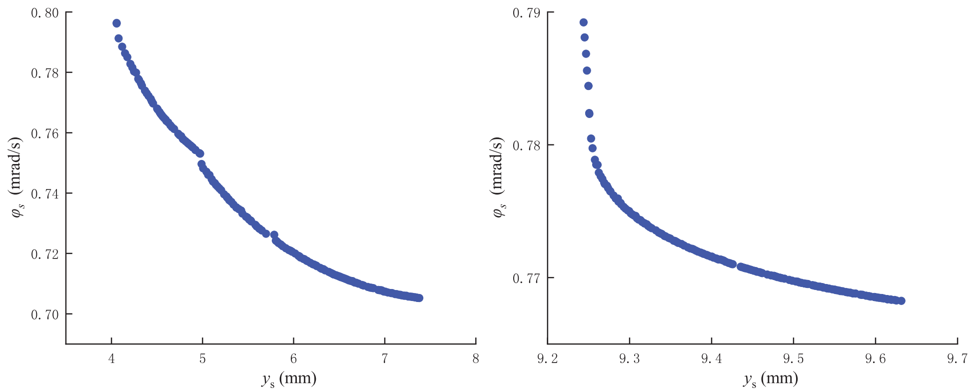

(a) The time delay is set as 0 (b) The time delay is set as 30ms

Figure 7. The Pareto front of multi-objective optimisation. (a) The time delay is set as 0; (b) The time delay is 30 ms.

Table 1. Optimised PID parameter.

Parameter	$\tau = 0$	$\tau = 30$ ms
k_p	0.193	188.627
k_i	46.856	42.933
k_d	45.733	0.730

time. Therefore, obtaining the minimum y_s and φ_s is contradictory to a certain extent. A set of parameters that ensures the relative balance can be obtained by multi-objective optimisation.

The NSGA-II algorithm is adopted to solve the multi-objective optimisation problem. The settings are chosen as the default except for the number of generations and population size. In this study, the number of generations is 100 and the population size is 2000.

4.3. *Multi-objective optimisation results*

Optimisation is performed for the situations with and without control delay. The Pareto fronts are shown in Figure 7. Figures show the contradiction between y_s and φ_s. When y_s reaches a better value, φ_s is correspondingly worse and vice versa. The control effect on lateral displacement is deeply affected by the control time delay τ of the controller. Instead, the influence of delay on the yaw angle is smaller. A set of PID parameters that can consider both y_s and φ_s are obtained through the Pareto front. The optimised parameters are shown in Table 1. With or without control delay, the parameters k_p and k_d are significantly different.

The results of linear analysis and time domain statistic simulation are shown in Figure 8.

It can be seen from Figure 8 that the magnitude of bogie frame lateral displacement is decreased under the PID control whether there is a delay or not in the theoretical model. Moreover, the magnitude of the yaw angle received influence from the control parameters. The formants of both lateral displacement and yaw angle are advanced under the effect of PID control because of the proportional part of the PID controller.

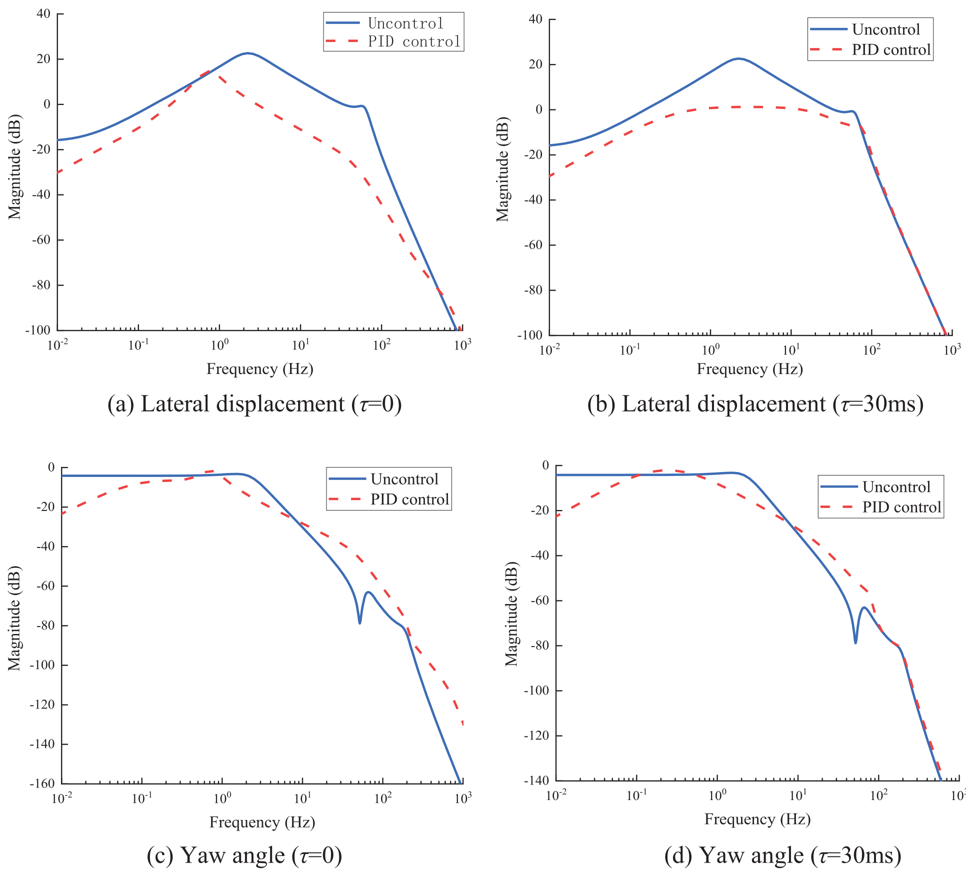

Figure 8. Transfer function (Bode diagram). (a) Lateral displacement ($\tau = 0$); (b) Lateral displacement ($\tau = 30$ ms); (c) Yaw angle ($\tau = 0$); (d) Yaw angle ($\tau = 30$ ms).

Table 2. Cases in controller setting.

Case	Delay	Control
1	×	×
2	×	○
3	○	○

Time domain integration is performed to obtain the whole six states of the bogie system under three cases. The operating speed is 360 km/h, simulation time is 8 s. Time domain results of bogie frame lateral displacement and yaw angle are shown in Figure 9. Details of three cases are shown in Table 2.

It can be illustrated from Figure 9(a) that the amplitude of bogie lateral displacement markedly decreased under the PID control whether with or without time delay. Moreover, the control effect without time delay is much better. The lateral vibration frequency of the bogie frame with delay is higher than that without delay, it is mainly due to the higher proportional gain in the PID algorithm. Figure 9(b) shows the bogie yaw damper curves in the three cases. The optimised performance of the yaw angle with or without time delay is similar, and the amplitude of which decreased correspondingly.

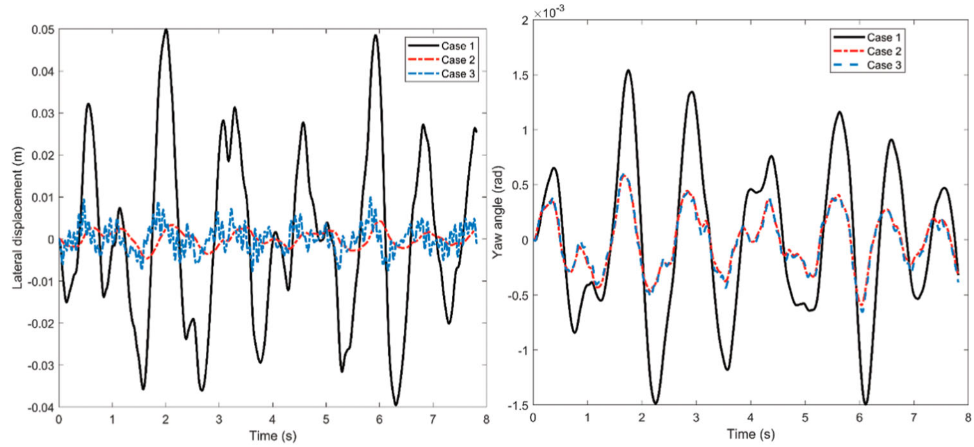

(a) Lateral displacement (b) Yaw angle

Figure 9. Time-domain results of the single bogie linear model. (a) Lateral displacement; (b) Yaw angle.

5. Vehicle dynamics co-simulation

5.1. Co-simulation model

The nonlinear vehicle model described in Section 2.2 is used for co-simulation between Simpack and Simulink to examine the control effect of optimised PID control in the SIMAT interface of Simulink. The linear model for control parameters optimisation is one bogie in the whole vehicle multibody dynamics model. Outputs of the vehicle model in the Simpack code are the lateral displacement and yaw angle of the two bogies. The output signals are delivered into the PID modulus to calculate the control force. After a delay of 30 ms measured in Section 4.1, the control force signals are sent back to the Simpack code as inputs of the four actuator force elements and acted between the car body and bogie in the model.

5.2. Co-simulation results

Two sets of PID parameters have been obtained in Section 4.2, one of which is the optimised PID setting without consideration of control delay, and the other is the optimised PID setting considering control delay. Co-simulation in this study is carried out in the three cases, as shown in Table 2. To make an unbiased comparison, the parameters in the three cases are the same except for the gain of PID controllers.

The operating speed of the vehicle is 360 km/h, and the simulation time is 9 s. Part of the simulation results is plotted to show the control effects in Figure 10. Some indexes are calculated and listed in Table 3.

An uncontrolled model is performed in case 1, which is set for the comparison of dynamic performance before and after control. Parameters in case 2 are optimised by the linear model without considering the control delay. On the contrary, the parameters in case 3 are optimised by the linear model with a delay of 30 ms.

Figure 10(a–d) shows the lateral acceleration and yaw angle acceleration of the car body and bogie frame in the time domain. Due to the influence of control delay, the control effects, when adopting optimal parameters without considering control delay, are not as

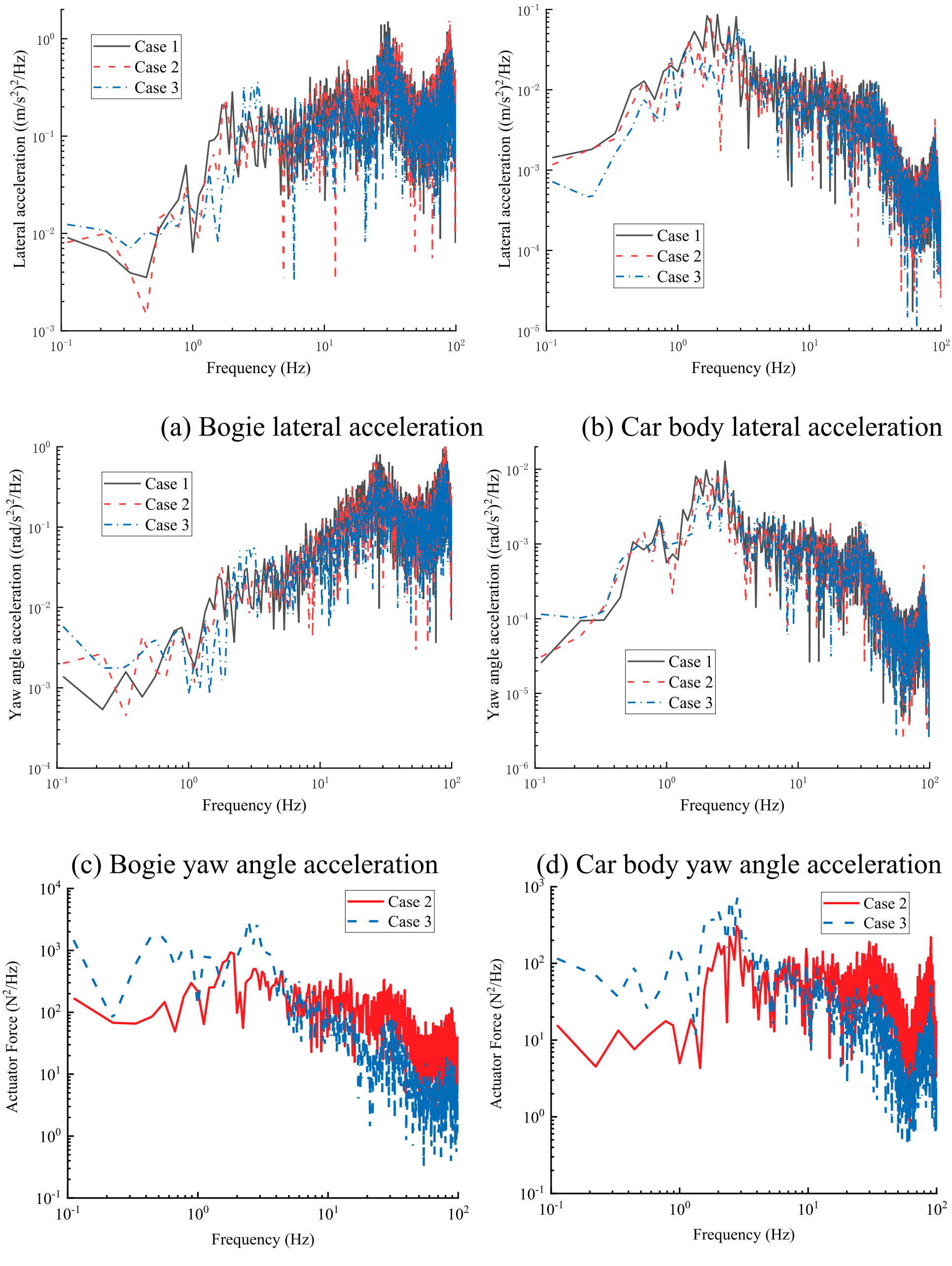

(a) Bogie lateral acceleration (b) Car body lateral acceleration

(c) Bogie yaw angle acceleration (d) Car body yaw angle acceleration

(e) Front-front actuator force (f) Rear-rear actuator force

Figure 10. Vehicle dynamics co-simulation results. (a) Bogie lateral acceleration; (b) Car body lateral acceleration; (c) Bogie yaw angle acceleration; (d) Car body yaw angle acceleration; (e) Front-front actuator force; (f) Rear-rear actuator force.

Table 3. Dynamic indexes in co-simulation.

Index	Case 1	Case 2	Case 3
RMS of bogie lateral acceleration	7.92 m/s^2	7.72 m/s^2	6.07 m/s^2
Car body lateral ride index	2.20	2.05	1.90
RMS of bogie yaw angle acceleration	5.34 rad/s^2	4.73 rad/s^2	3.82 rad/s^2
RMS of car body yaw angle acceleration	0.0219 rad/s^2	0.0197 rad/s^2	0.0170 rad/s^2
RMS of bogie lateral displacement	3.54 mm	2.80 mm	2.51 mm
RMS of car body lateral displacement	2.62 mm	2.35 mm	1.92 mm

good as the optimisation results in the linear model. Control performance considering the time delay is much better. When time delay exists and not be considered as Case 2, the control effect is not good enough that the dynamic performance is not obviously improved compared with that in the vehicle with passive suspension. When considering the time delay in optimisation as in Case 3, the lateral stability of the car body is obviously improved in the low-frequency range, but the lateral vibration of the frame deteriorates at 2–4 Hz.

The force of actuators is analysed to evaluate the behaviours of actuators in case 2 and case 3. Figure 10(e,f) illustrates the active control force in the front beam of the front bogie frame and the rear beam of the rear bogie frame in the frequency domain. The difference between actuator force curves in the two cases is significant. In case 2, the actuator force is distributed relatively evenly in each frequency band, with only small peaks near the hunting frequency of the car body and bogie. The actuator force curves in case 3 only show a significant peak near the car body hunting frequency, while the force at other frequencies is relatively small. The delay of 30 ms will lead to the phase difference of the active force. The higher the frequency, the worse the real-time performance of the actual force control, and the worse the control effect. Based on the above analysis, the parameter set in case 3 is more effective in eliminating the lateral displacement of both the bogie frame and car body in a control system with time delay.

6. HIL simulation validation

6.1. HIL simulation system

Based on the dynamic characteristics of actuators and the force feedback control in Section 3, an inertial actuator in HIL simulation containing, a vehicle dynamics simulation model in the Concurrent Workbench platform and inertial actuators with the real-time control system is established, where the inertial actuators and the control system are physical hardware. Concurrent Workbench is a kind of real-time simulation computer whose calculation speed is fast enough to ensure real-time performance for hardware-in-the-loop simulation. The vehicle model in the loop is established using the Simpack code described in Section 2.

In the process of HIL simulation, the vehicle model is saved as an RTDB (Real-Time DataBase) library and transported to the Concurrent Workbench as the computational model. The lateral displacement of two bogies is set as output variables of the simulation workbench, and the inertial forces of actuators are set as the inputs. Data exchange between Concurrent Workbench and controller is through the router following User Datagram Protocol(UDP). A lower computer and an I/O device participate in the HIL simulation circuit as the controller of inertial actuators and the data collector. Lateral displacement from the computer is calculated by the PID algorithm and the actuator force feedback algorithm is

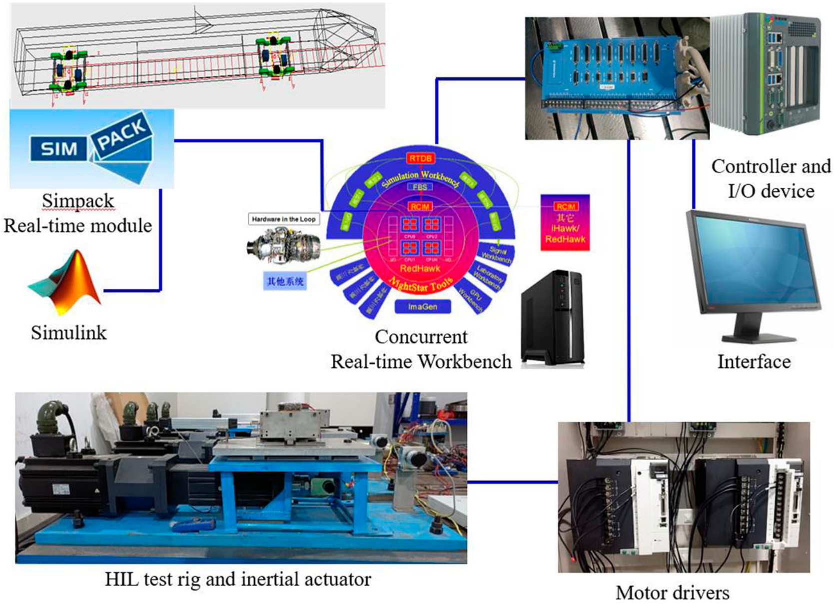

Figure 11. Configuration of HIL simulation.

written into the lower computer before generating the actuating signals for the actuators. Voltage signals from the sensors are collected by the lower computer and interpreted into unified form then conducted to the simulation computer as force inputs. At this point, a loop consisting of the simulation workbench, the lower computer and the actuators are formed, and the simulation is completed through data exchange in the established cycle (Figure 11).

6.2. HIL simulation results

According to the previous simulation results, the actuator set in the rear end of the bogie frame is required to generate a smaller force. To achieve a more relatively realistic simulation with limited conditions, two physical actuators are set as the force elements in both front ends of two bogies, and actuators in two rear ends are regarded as ideal force elements only with time delay. Working condition settings are the same as those in the SIMAT simulation. To protect the test equipment from collision, the track excitation setting is smaller than that in the SIMAT simulation. Car body lateral acceleration and actuator force in two beams of the vehicle in the HIL simulation are extracted and plotted in Figure 12.

The lateral ride indexes of the car body under cases 1–3 are 2.16, 1.96 and 1.81, respectively, and after the active control force is applied, the lateral vibration problem of the car body is significantly improved, and compared with the case 2 that does not consider the impact of the time delay, the case 3 that considers the time delay shows a better control effect. Due to the time delay and inevitable errors in the hardware test, the HIL simulation results are slightly different from the statistic simulation results, but the overall change trend is consistent, and in general, the two results are basically the same. The conclusion

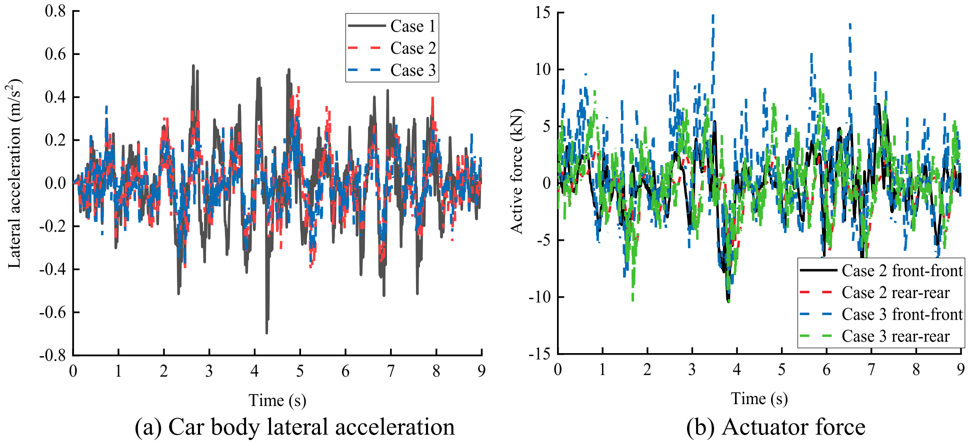

Figure 12. HIL simulation results. (a) Car body lateral acceleration; (b) Actuator force.

can be drawn that applying the optimised parameters considering a delay to the HIL simulation can obtain a better experimental performance than using the optimised parameters from an idealised model. The results of the above research will subsequently offer guidance for practical operations.

7. Conclusion

(1) Dynamic characteristics of a type of inertial actuator and the feedback control strategies are studied and tested in the experiment. As a result, linear force feedback is the most straightforward and effective method for the force-tracking of the inertial actuator. By adopting the linear force feedback control, the inertial actuator can be regarded as an ideal force element in the upper controller.

(2) To enhance the hunting stability the multi-objective control parameters' optimisation with reducing lateral displacement and yaw angle of the bogie frame is performed on an active linear bogie model with the consideration of the dynamic response of the inertial actuator. In the linear bogie model, two inertial actuators are mounted on the front and end beams of the bogie frame as generators of active control force. The time delay of 30 ms in the actual control system is measured by experiment. The results indicate that the optimised PID control parameters are obviously different in the model with or without time delay. The lateral vibration intensity of the bogie frame increases caused by the time delay. On the contrary, the influence on the yaw vibration amplitude is much smaller.

(3) The active stability effects are validated through the vehicle dynamics co-simulation and the inertial actuator control system in the HIL simulation. Active force should concentrate more on the low-frequency domain and the performance at high frequencies can be easily affected by the time delay in an active control system. By comparing the dynamic performances of vehicle models on a straight track in three cases of control setting, the PID parameters optimised by the proposed method can obtain better performance in practical situations.

Disclosure statement

No potential conflict of interest was reported by the author(s)

Funding

The material in this paper is based on work supported by the Natural Science Foundation of Sichuan Province (2022NSFSC0034, 2022NSFSC1901) and National Railway Group Science and Technology Program grant (N2020J028) and Traction Power State Key Laboratory grant (2022TPL_T02, TPL2006) of the Independent Research and Development Projects.

ORCID

Yuan Yao http://orcid.org/0000-0003-2279-7463

References

[1] Goodall RM, Kortüm W. Mechatronic developments for railway vehicles of the future. Control Eng Pract. 2002;10(8):887–898.
[2] Foo E, Goodall RM. Active suspension control of flexible-bodied railway vehicles using electro-hydraulic and electro-magnetic actuators. Control Eng Pract. 2000;8(5):507–518.
[3] Ward CP, Weston PF, Stewart EJC, et al. Condition monitoring opportunities using vehicle-based sensors. P I Mech Eng F-J Rai. 2011;225(F2):202–218.
[4] Yao Y, Zhang X, Liu X. The active control of the lateral movement of a motor suspended under a high-speed locomotive. P I Mech Eng F-J Rai. 2016;230(6):1509–1520.
[5] Yao Y, Wu G, Yousef S, et al. Hunting stability analysis of high-speed train bogie under the frame lateral vibration active control. Veh Syst Dyn. 2018;56(2):297–318.
[6] Hou Y, Song Y, Wu G, et al. Simulation and experimental study on the active stability of high-speed trains. Comput Sci Eng. 2019;21(3):72–82.
[7] Park J, Shin Y, Hur H, et al. A practical approach to active lateral suspension for railway vehicles. Meas Control-UK. 2019;52(9-10):1195–1209.
[8] Yao Y, Li G, Yousef S, et al. Stability enhancement of a high-speed train bogie using active mass inertial actuators. Veh Syst Dyn. 2019;57(3):389–407.
[9] Jin T, Liu Z, Sun S, et al. Development and evaluation of a versatile semi-active suspension system for high-speed railway vehicles. Mech Syst Signal Pr. 2020;135:106338.
[10] Zhang X, Wu G, Li G, et al. Actuator optimal placement studies of high-speed power bogie for active hunting stability. Veh Syst Dyn. 2020;58(1):108–122.
[11] Khadr A, Houidi A, Romdhane L. Design and optimization of a semi-active suspension system for a two-wheeled vehicle using a full multibody model. P I Mech Eng K-J Mul. 2017;231(4):630–646.
[12] Qazizadeh A, Stichel S, Feyzmahdavian H. Wheelset curving guidance using H-infinity control. Veh Syst Dyn. 2018;56(3):461–484.
[13] Jiang JJ, Matamoros A, Goodall RM, et al. Passive suspensions incorporating inerters for railway vehicles. Veh Syst Dyn. 2012;50(sup1):263–276.
[14] Matamoros A, Goodall RM, Zolotas A, et al. Stability control of a railway vehicle using absolute stiffness and inerters. In: Proceedings of 2012 UKACC International Conference on Control; Cardiff, UK; 2012. p. 120–127.
[15] Wang FC, Hsieh MR, Chen HJ. Stability and performance analysis of a full-train system with inerters. Veh Syst Dyn. 2012;50(4):545–571.
[16] Braghin F, Cinquemani S, Resta F. A low frequency magnetostrictive inertial actuator for vibration control. Sensor Actuat A-Phys. 2012;180:67–74.
[17] Benassi L, Elliott SJ, Gardonio P. Active vibration isolation using an inertial actuator with local force feedback control. J Sound Vib. 2004;276(1–2):157–179.

[18] Benassi L, Elliott SJ. Active vibration isolation using an inertial actuator with local displacement feedback control. J Sound Vib. 2004;278(4–5):705–724.
[19] Borgo MD, Ghandchi-Tehrani M, Elliott SJ. Identification and analysis of nonlinear dynamics of inertial actuators. Mech Syst Signal Pr. 2019;115:338–360.
[20] Rulka W, Pankiewicz E. MBS approach to generate equations of motions for HiL-simulations in vehicle dynamics. Multibody Syst Dyn. 2005;14(3-4):367–386.
[21] Kim SS, Jeong W. Subsystem synthesis method with approximate function approach for a real-time multibody vehicle model. Multibody Syst Dyn. 2007;17(2-3):141–156.
[22] Spiryagin M, Sun YQ, Cole C, et al. Development of a real-time bogie test rig model based on railway specialised multibody software. Veh Syst Dyn. 2013;51(2):236–250.
[23] Batterbee DC, Sims ND. Hardware-in-the-loop simulation of magnetorheological dampers for vehicle suspension systems. P I Mech Eng I-J Sys. 2007;221(I2):265–278.
[24] Zhang XM, Wu M, She J, et al. Delay-dependent stabilization of linear systems with time-varying state and input delays. Automatica (Oxf). 2005;41(8):1405–1412.
[25] Chen B, Liu XP, Tong SC, et al. Observer-based stabilization of T-S fuzzy systems with input delay. IEEE T Fuzzy Syst. 2008;16(3):652–663.
[26] Shin D, Lee G, Yi K, et al. Motorized vehicle active suspension damper control with dynamic friction and actuator delay compensation for a better ride quality. P I Mech Eng D-J Aut. 2016;230(8):1074–1089.
[27] Bideleh SSM, Mei TX, Berbyuk V. Robust control and actuator dynamics compensation for railway vehicles. Veh Syst Dyn. 2016;54(12):1762–1784.

Appendix

$$\mathbf{M}_\mathrm{b} = \begin{bmatrix} m_w & & & & & \\ & I_w & & & & \\ & & m_w & & & \\ & & & I_w & & \\ & & & & m_f & \\ & & & & & I_f \end{bmatrix}$$

$$\mathbf{C}_\mathrm{b} = \begin{bmatrix} \frac{2f_\eta}{v} & & & & & \\ & \frac{2l_0^2 f_\zeta}{v} & & & & \\ & & \frac{2f_\eta}{v} & & & \\ & & & \frac{2l_o^2 f_\zeta}{v} & & \\ & & & & l_2^2 c_{sx} & \\ & & & & & l_2^2 c_{sx} \end{bmatrix}$$

$$\mathbf{K}_\mathrm{b} = \begin{bmatrix} k_{py}+k_{gy} & -2f_\eta & & & -k_{py} & -bk_{py} \\ \dfrac{2\lambda l_0 f_\zeta}{r_0} & l_1^2 k_{px}+k_{g\psi} & & & & -l_1^2 k_{px} \\ & & k_{py}+k_{gy} & -2f_\eta & -k_{py} & bk_{py} \\ & & \dfrac{2\lambda l_0 f_\zeta}{r_0} & l_1^2 k_{px}+k_{g\psi} & & -l_1^2 k_{px} \\ -k_{py} & & -k_{py} & & 2k_{py}+k_{sy} & \\ -bk_{py} & -l_1^2 k_{px} & bk_{py} & -l_1^2 k_{px} & & l_2^2 k_{sx}+2l_1^2 k_{px}+2b^2 k_{py} \end{bmatrix}$$

$$\mathbf{B} = \begin{bmatrix} 0 & 0 & 0 & 0 & 1 & l_m \\ 0 & 0 & 0 & 0 & 1 & l_m \end{bmatrix}^\mathrm{T}$$

$$\mathbf{w} = \begin{bmatrix} k_{py} & 0 & k_{py} & 0 & 0 & 0 \end{bmatrix}^\mathrm{T}$$

Related parameters and its value

Parameter name	Symbol	Unit	Value
Mass of bogie frame	m_f	kg	2328
Mass of wheelset	m_w	kg	1639
Moment of inertia around *z* axle of bogie frame	I_f	kg m^2	4080
Moment of inertia around *z* axle of wheelset	I_w	kg m^2	822
Stiffness of primary longitudinal suspension	k_px	kN/m	120,000
Stiffness of primary lateral suspension	k_py	kN/m	12,500
Stiffness of secondary longitudinal suspension	k_sx	kN/m	66.5
Stiffness of secondary lateral suspension	k_sy	kN/m	66.5
Damping coefficient of secondary longitudinal suspension	c_sx	kN s/m	330
Damping coefficient of secondary lateral suspension	c_sy	kN s/m	15
Half of the distance between primary lateral dampers	l_1	m	1
Half of the distance between secondary lateral dampers	l_2	m	0.95
Half of bogie wheelbase	b	m	1.25
Radius of wheelset	r_0	m	0.46
Equivalent conicity	λ	–	0.18